Plasmonics (2012) 7:739–744
DOI 10.1007/s11468-012-9366-0

Distance Dependence of Metal-Enhanced Fluorescence

Anatoliy I. Dragan · Eric S. Bishop · Jose R. Casas-Finet · Robert J. Strouse · James McGivney · Mark A. Schenerman · Chris D. Geddes

Received: 23 June 2011 / Accepted: 20 April 2012 / Published online: 12 May 2012

Abstract In recent years both the mechanism and applications of metal-enhanced fluorescence (MEF) have attracted significant attention, yet many fundamental aspects of MEF remain unanswered or addressed. In this study, we address a fundamental aspect of MEF. Using fluorescein-labeled different length DNA scaffolds, covalently bound to silver nanodeposits, we have experimentally measured the distance dependence of the MEF effect. The enhanced fluorescence signatures, i.e., MEF, follow quite closely the theoretical decay of the near-field of the nanoparticles, calculated using finite difference time domain approaches. This implies that the mechanisms of MEF are partially underpinned by the magnitude and distribution of the electric field around near-field nanoparticles.

Keywords Metal-Enhanced fluorescence · Surface plasmons · Near-field strength · Nanoparticles · DNA scaffolds · Surface-enhanced fluorescence · Radiative-decay engineering · Plasmon-enhanced fluorescence

A. I. Dragan · C. D. Geddes (✉)
Institute of Fluorescence and Department of Chemistry and Biochemistry, The Columbus Center,
University of Maryland Baltimore County,
701 East Pratt Street,
Baltimore, MD 21202, USA
e-mail: Geddes@umbc.edu

E. S. Bishop · J. R. Casas-Finet · R. J. Strouse · J. McGivney · M. A. Schenerman
MedImmune LLC,
1 MedImmune way,
Gaithersburg, MD 20878, USA

Introduction

In the last 10 years, Metal-Enhanced Fluorescence has emerged as a nanotechnology which looks set to change how we both use and think about fluorescence spectroscopy today. In the near-field, i.e., less than one wavelength away, fluorophore dipoles can interact with plasmon supporting materials in ways which increase fluorophore brightness and enhance photostability, enhance chemiluminescence signatures, generate enhanced singlet oxygen, and superoxide anion radical, to name but just a very few applications [1–3]. In more recent years, Geddes has postulated the underlying two mechanisms of MEF: (a) an enhanced excitation rate or enhanced absorption cross-section, and (b) how mirror dipoles are formed on nanoparticles, the amplified confined and frequency specific resonances eventually radiated by the nanoparticles themselves. This is in contrast to the more simplistic radiative rate model postulated by others [4]. In addition, the wavelength dependence of metal-enhanced fluorescence has also been recently postulated [5], which suggests that MEF is partly underpinned by the spectral overlap of a fluorophores' emission spectra with the scattering component/s of the nanoparticles' extinction spectra. MEF parameters of dye/nanoparticle coupled system, in particular, are related to the distribution of the near-field intensity and its distance-dependent decay function. During decades there were many attempts to measure enhancement factors and the dependence of the fluorescence enhancement parameters upon the distance from a metal surface in macrosystem, which has included metal deposits, spacers of different nature and dye solutions, [6–9] and in single-molecule system [10, 11]. While these parameters are phenomenologically known, it is still not possible to reliably predict actual far-field fluorescence enhancement factors, which is the ultimate goal for the potential downstream

(a) 50 b ssDNA:

SH-$(CH_2)_6$-5′-**GAG ATA TGA GCA AAA GAA ACT TGG AAA GGA GGC TGG AGA GAT GGC TCG AG**

(b) 57 b ssDNA:

SH-$(CH_2)_6$-5′-**C TTT TTA GAG ATA TGA GCA AAA GAA ACT TGG AAA GGA GGC TGG AGA GAT GGC TCG AG**

(c) A series of short ssDNA, labeled with FAM, used for hybridization with 50 b or 57 b ssDNA:

50 bp **FAM-5′-DNA:**
SH-$(CH_2)_6$-5′-**GAG ATA TGA GCA AAA GAA ACT TGG AAA GGA GGC TGG AGA GAT GGC TCG AG**
CTC TAT ACT CGT TTT CTT TGA ACC TTT CCT CCG ACC TCT CTA CCG AGC TC-**FAM**

39 bp **FAM-5′-DNA:**
SH-$(CH_2)_6$-5′-**GAG ATA TGA GCA AAA GAA ACT TGG AAA GGA GGC TGG AGA GAT GGC TCG AG**
CTC TAT ACT CGT TTT CTT TGA ACC TTT CCT CCG ACC TCT-**FAM**

30 bp **FAM-5′-DNA:**
SH-$(CH_2)_6$-5′-**GAG ATA TGA GCA AAA GAA ACT TGG AAA GGA GGC TGG AGA GAT GGC TCG AG**
CTC TAT ACT CGT TTT CTT TGA ACC TTT CCT-**FAM**

19-20 bp FAM-5′-DNA :
SH-$(CH_2)_6$-5′-**GAG ATA TGA GCA AAA GAA ACT TGG AAA GGA GGC TGG AGA GAT GGC TCG AG**
CTC TAT ACT CGT TTT CTT T-FAM

39 bp **DNA-3′-FAM:**
SH-$(CH_2)_6$-5′-**GAG ATA TGA GCA AAA GAA ACT TGG AAA GGA GGC TGG AGA GAT GGC TCG AG**
FAM-T TTT CTT TGA ACC TTT CCT CCG ACC TCT CTA CCG AGC TC

49 bp **DNA-3′-FAM :**
SH-$(CH_2)_6$-5′-**GAG ATA TGA GCA AAA GAA ACT TGG AAA GGA GGC TGG AGA GAT GGC TCG AG**
FAM-TC TAT ACT CGT TTT CTT TGA ACC TTT CCT CCG ACC TCT CTA CCG AGC TC

Fig. 1 **a, b** The 50 b or 57 b ssDNA was attached to silver NPs. **c** The DNA duplexes formed on SiFs after annealing short FAM-labeled ssDNA oligos with DNA attached to SiFs. The distance from the SiF surface to FAM, attached to DNA, varies from 2 nm (49b/50b duplex) to 20 nm (50b/57b duplex)

utility of MEF in the Biosciences. In this paper we subsequently extend our current thinking of MEF phenomena and show that the *distance dependence* of MEF enhancement follows closely the near-field electric field distribution around nanoparticles. Hence, experimentally determined enhanced fluorescence values for fluorophores, located at defined distances from nanoparticles using DNA scaffolds, are shown to correlate very well with theoretically determined electric field distributions determined using the finite difference time domain numerical method, in a way that suggests that luminescence enhancement factors can be approximated by the decay of the near-field. Our findings are not only significant for the continued development of a theoretical framework for MEF, but also for its multifarious applications in the biosciences [3, 12–16].

Materials and Methods

Silver nitrate (99.9 %), sodium hydroxide (99.996 %), ammonium hydroxide (30 %), D-glucose and premium quality APS-coated glass slides (75×25 mm) were obtained from Sigma-

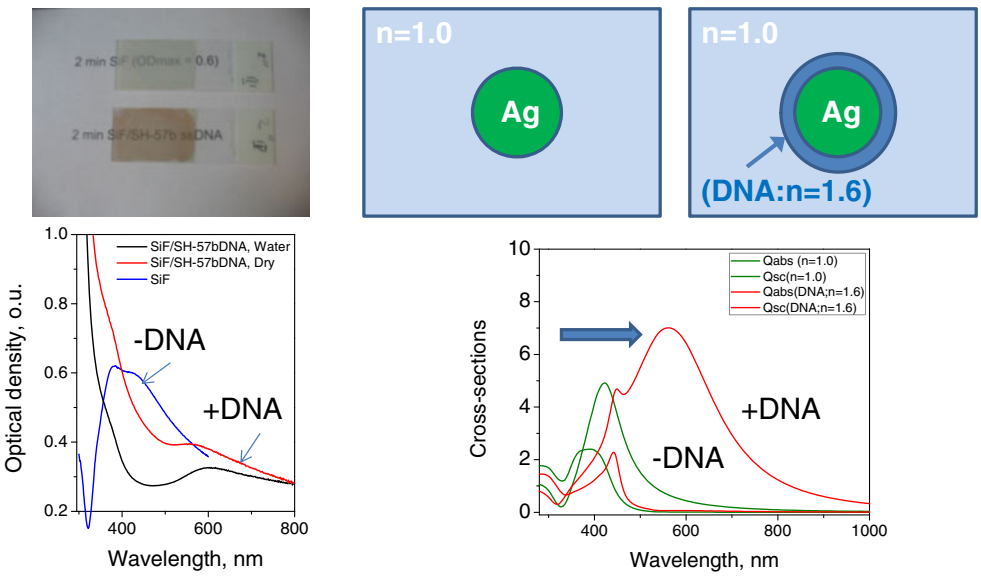

Fig. 2 (*Left, top*) Photographs of SiF slides before (*Top*) and after (*Bottom*) DNA attachment to SiFs. (*Left, bottom*) Absorption spectra of a dry silver island film (SiF), dry and wet SiF, after attachment of the SH-57b ssDNA. (*Right, top*) Cartoons depicting a silver NP in air (refractive index, $n=1.0$) and for a nanoparticle surrounded by DNA with a refractive index of $n=1.6$. (*Right, bottom*) Results of Mie theory calculations: Absorption and scattering spectra of 100 nm Ag-NP in air ($n=1.0$); 100 nm Ag-NP surrounded by 25 nm DNA-shell ($n=1.6$)

Aldrich. The DNA sequences used in this study are fragments of Chinese hamster ovary (CHO) Alu sequence. Oligonucleotides were purchased from Integrated DNA Technologies, Inc.

DNA scaffolds, Fig. 1, were designed using CHO sequences, such that upon specific hybridization, a fluorescent label is rigidly positioned above silver-island nanodeposits (SiFs), the distance varies from 2 to 20 nm, Fig. 1. The preparation of silver-island nanodeposits has been described elsewhere [17]. The 5′-sulfhydral terminated DNA (5′-SH-DNA) was incubated on SiFs for the anchoring of the DNA to the surface as described in [18]. This typically resulted in a broadening of the SiFs absorption spectrum, which could readily be explained by a change in the refractive index above the metal as theoretically modeled and confirmed using Mie simulations, Fig. 2. The addition of DTT (dithiotreitol), after complimentary DNA annealing and enhanced fluorescence (due to the proximity of the FAM label to SiFs), confirmed that the DNA was anchored as the sulfhydral-silver bond was both reduced and broken as evidenced by the loss of enhanced fluorescence, Fig. 3. Interestingly, this novel but simplistic approach allows one to readily determine fluorescence enhancement factors, which is particularly important as a control sample and when 5′-SH-DNA does not bind to glass or indeed other substrates. After hybridization, the fluorescent label FAM was exited using a 473 nm CW laser line and the emission collected through a notch filter, falling incident on a 600 μm fiber bundle and an Ocean-Optics HD-2000 spectrometer. Theoretical electric field distributions were determined using the finite difference time domain method which has been described in detail elsewhere [19].

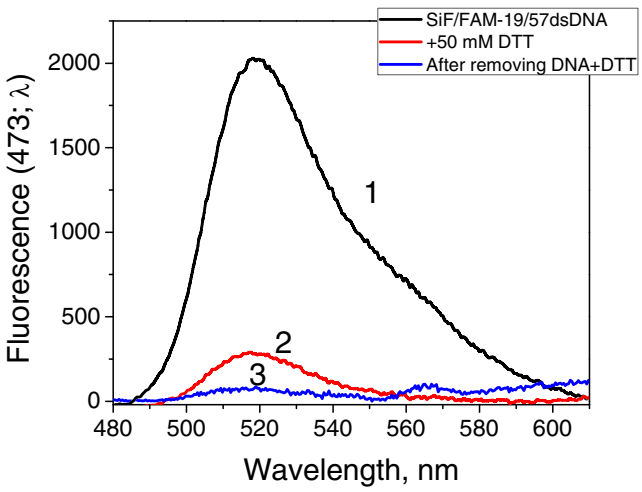

Fig. 3 (*1*) Fluorescence spectra of FAM-DNA, attached to SiFs, (*2*) FAM-DNA fluorescence after addition of reducing agent (50 mM DTT) and incubation for 30 min, and (*3*) fluorescence after removing DTT-containing solution. *DTT* dithiotreitol

Results

Figure 4, top shows a typical E-Field distribution around a 100 nm nanoparticle, a size typical for SiF's as recently reported by our group [17]. By taking a line-scan through the *y*-plane, one is able to generate a plot of the field decay from the nanoparticles' surface, Fig. 4, bottom, open circles. Interestingly, an overlaid normalized plot of near-field *enhanced* fluorescence from the DNA-fluorophore scaffolds after annealing, shows an almost identical trend (solid circles). This suggests that the enhanced fluorescence decreases exponentially from the surface in an analogous manner to

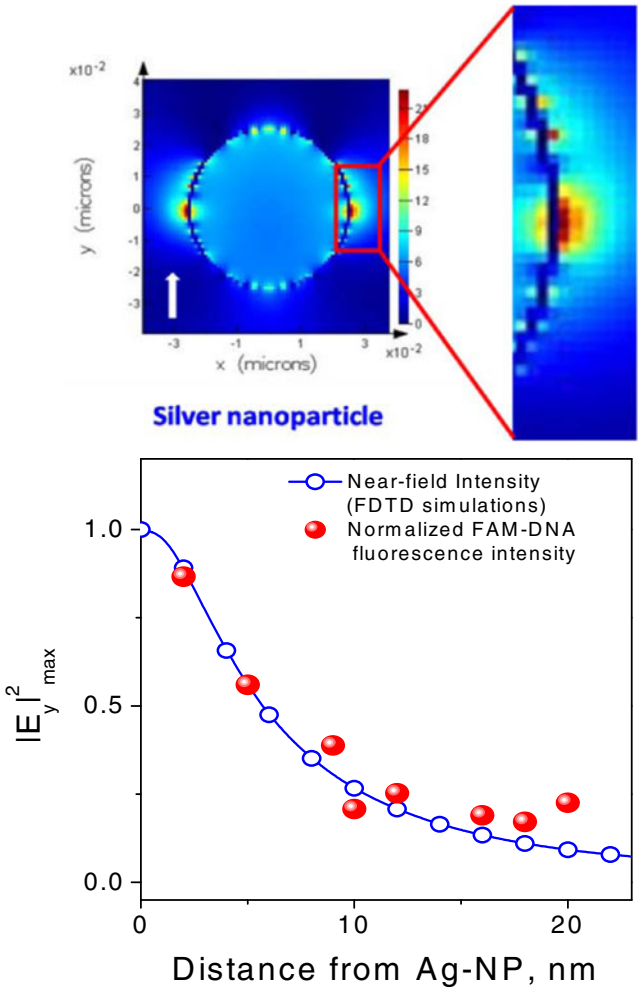

Fig. 4 (*Top*) Simulated distribution of the E-field (*y*-plane) around a silver NP, induced by incident light at 468 nm. (*Top, right*) Enlarged view of the near-field formed near-to the surface of the silver NP. (*Bottom*) Calculated dependence of the near-field intensity upon the distance from the NP surface (*open circles*) and the normalized observed fluorescence intensity from different FAM-DNAs, attached to SiFs, that are characterized by different distances of FAM to the silver surface (*solid red circles*). *NP* nanoparticle

Table 1 Results of FAM-DNA fluorescence decay analysis

Fitting conditions	Distance, nm	A_1	τ_1, ns	A_2	τ_2, ns	A_3	τ_3, ns	$<\tau>$, ns	χ^2
Three exponents	2	−54.15	0.49	54.21	0.49	0.46	4.57	2.14	6.15
	5	−51.61	0.49	52.15	0.49	0.47	4.71	2.77	6.65
	7	−4.64	0.45	5.19	0.51	0.44	4.52	2.57	6.4
	18	−1606.7	0.46	1607.3	0.46	0.43	4.58	2.55	7.2
Two exponents	2	–	–	0.42	0.68	0.58	3.2	2.14	1.05
	5	–	–	0.41	0.67	0.59	3.2	2.16	1.05
	7	–	–	0.46	0.67	0.53	3.2	2.02	1.4
	18	–	–	0.45	0.64	0.55	3.03	1.94	1.2
Free space	∞	–	–	0.59	3.5	0.45	4.85	4.25	1.1

Fluorescence decay functions were fitted by three components, including the rise time, and by two components, omitting the rise time. In both cases, DNA of different length, labeled with FAM (see Fig. 1) was attached to SiFs surface through DNA 5′-SH group. Distances from the chromophore to the SiFs surface are simply calculated using the length of DNA between labeled nucleotide and 5′-SH group. The last row shows deconvolution of fluorescence decay of FAM-DNA free in solution fitted to a 2-exponential function

the exponential electric field near-field decay above the surface. MEF is thought to be underpinned by two complimentary but different mechanisms [1], an enhanced absorption and an enhanced emission component. Subsequently, our findings suggest that both mechanisms of enhancement follow the same exponential distance dependence. It is also important to note that other groups, in addition to ours, have also studied the distance dependence of MEF, but in these other studies, fluorophore solutions randomly oriented above nanoparticles have provided for heterogeneous distance distribution functions [7, 20], giving limited information on the underlying coupling of fluorophores to plasmon supporting nanoparticles.

We also estimated total fluorescence enhancement of the dye at short distances from NPs. For that we have measured enhancement of fluorescein (fluorescein-labeled DNA free in solution) fluorescence on SiFs relative to glass (control), MEF is about ≈10. Attachment of labeled DNA to SiFs causes additional enhancement of fluorescein fluorescence, e.g. enhancement of approximately eightfold we have measured for 19 b DNA-linker (dye-metal distance D≈10 nm), Fig. 3. In total, relative to the glass control, the MEF effect for fluorescein attached to SiFs by 19 b DNA linker is around 80. Subsequently, at shorter distances total enhancement could reach MEF≈360, at D=2 nm (see Fig. 4).

Reduced fluorophore decay times are frequently reported in MEF [3], and are thought to reflect the more rapid system coupled lifetime as compared to the lifetime of the free-space fluorophore [1, 3, 12]. For our FAM-DNA scaffolds we see that the amplitude weighted lifetimes are much shorter, around 2.14 ns, as compared to the free-space lifetime of 4.25 ns, consistent with other MEF reports, Table 1. Interestingly, a rise time in the time-resolved intensity decays appears to be present for the DNA scaffolds, Fig. 5 right, as compared to the control sample, left, suggesting the energy pumping of surface plasmons by the fluorophore, consistent with current MEF thinking that fluorophores form a mirror dipole in the near-field

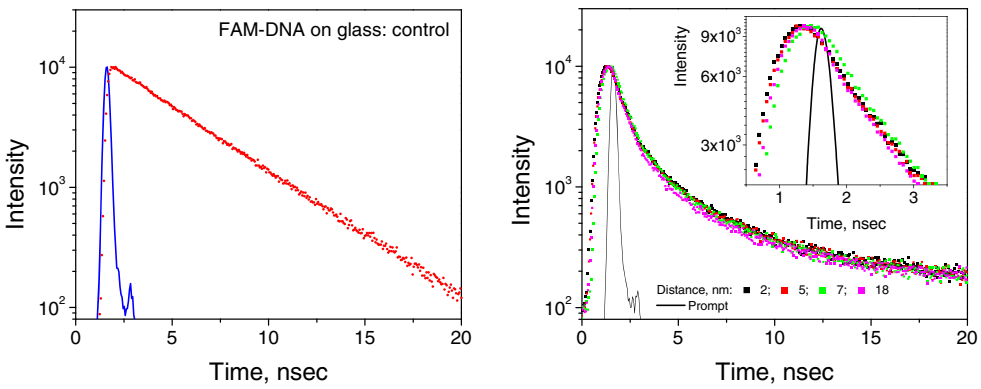

Fig. 5 (*Left*) Fluorescence decay curve of FAM-labeled DNA on glass (control). (*Right*) Fluorescence decay curves of FAM-labeled DNAs attached to SiFs. The distance of FAM to the silver surface was: 9, 13, 16, and 20 nm. Excitation of fluorescence was undertaken using a 444 nm laser line

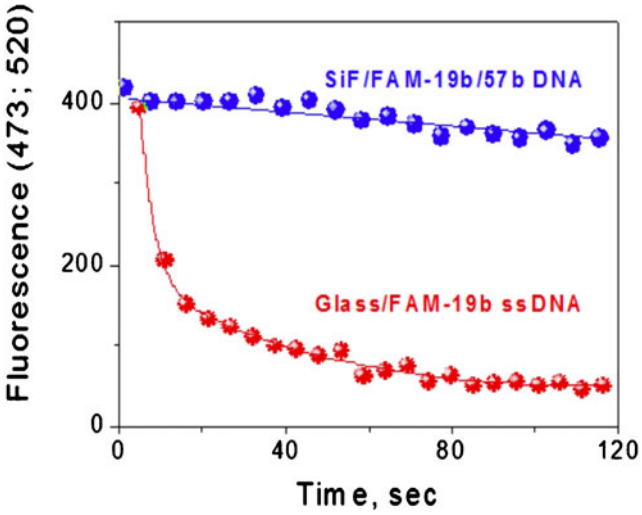

Fig. 6 Photobleaching (intensity versus time) of FAM-labeled DNA, attached to SiFs, and in bulk solution upon 473 nm laser irradiation. Laser power was 50 mW. Buffer: TE, pH 7.6

[1], i.e., non-radiative transfer from the fluorophore to the metal.

It is well-known that a fluorophore's photostability is underpinned by its lifetime [2–4], where longer fluorescence lifetimes provide for greater opportunities for excited state destructive photophysics. Figure 6, shows the intensity vs. time (photostability) of the FAM-DNA (19/57 base-pair) scaffold as compared to the same but using a glass control sample containing no silver, the sample geometry shown in Fig. 7. Quite notably, there is a significant difference in FAM photostability, where considerably more photons per unit time (photon flux) is observed from the silvered substrate supporting the DNA scaffolds, suggesting that DNA-fluorophore scaffolds can be readily constructed on silvered substrates for both enhanced fluorophore photostabilities and predictive luminescence enhancement.

In closing, we have studied the enhanced fluorescence of FAM-DNA scaffolds on silver nanodeposits and can show that the enhanced fluorescence signatures, i.e., MEF, follow quite closely the theoretical distance-dependent decay of the E-field intensity of the nanoparticles at the excitation wavelength. Fundamentally, this implies that both mechanisms in MEF are partially determined by the magnitude and distribution of the +electric field around nanoparticles. In addition, a rise time in the time-resolved decay data strongly suggests fluorophore energy pumping of the metal surface plasmons, consistent with current MEF thinking [1, 3]. Remarkably, our results suggest that one may well be able to predict near-field fluorescent enhancement factors, albeit in a relativistic fashion, which is a significant advance over the current state-of-the art in the MEF literature [3].

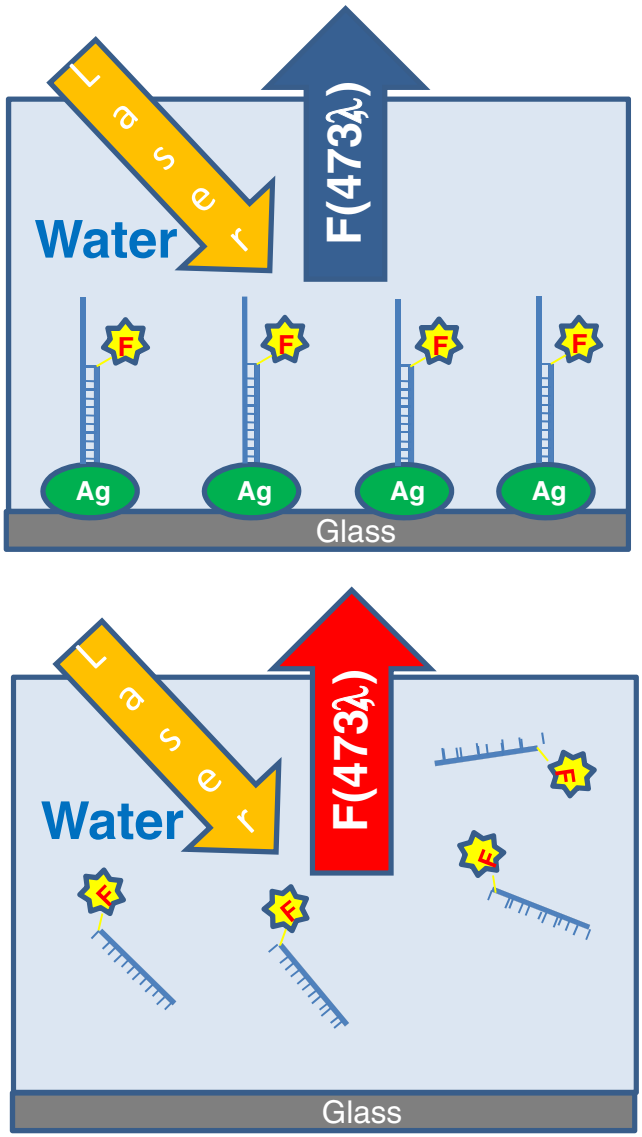

Fig. 7 Cartoon depicting two different experimental geometries to study FAM-DNA photostability: FAM-DNA, attached to SiFs (*top*) and free in solution (*bottom*). The same concentration of DNA was used in each geometry

Acknowledgments The authors thank MedImmune Inc., for financial support as well as the University of Maryland Baltimore County for salary contributions.

References

1. Aslan K, Geddes CD (2010) In: Geddes CD (ed) Metal-enhanced fluorescence: progress towards a unified plasmon-fluorophore description. Wiley, Hoboken, NJ, pp 1–24
2. Geddes CD, Lakowicz JR (2002) Metal-enhanced fluorescence. J Fluoresc 12(2):121–129
3. Geddes CD (2010) Metal-enhanced fluorescence. Wiley, Hoboken, NJ

4. Lakowicz JR (2006) Principles of fluorescence spectroscopy. Springer, New York
5. Zhang Y, Dragan A, Geddes CD (2009) Wavelength dependence of metal-enhanced fluorescence. J Phys Chem C 113(28):12095–12100
6. Kummerlen J et al (1993) Enhanced dye fluorescence over silver island films: analysis of the distance dependence. Mol Phys 80 (5):1031–1046
7. Ray K, Badugu R, Lakowicz JR (2007) Polyelectrolyte layer-by-layer assembly to control the distance between fluorophores and plasmonic nanostructures. Chem Mater 19(24):5902–5909
8. Ray K, Badugu R, Lakowicz JR (2007) Sulforhodamine adsorbed Langmuir–Blodgett layers on silver island films: effect of probe distance on the metal-enhanced fluorescence. J Phys Chem C Nanomater Interface 111(19):7091–7097
9. Sokolov K, Chumanov G, Cotton TM (1998) Enhancement of molecular fluorescence near the surface of colloidal metal films. Anal Chem 70(18):3898–3905
10. Anger P, Bharadwaj P, Novotny L (2006) Enhancement and quenching of single-molecule fluorescence. Phys Rev Lett 96 (11):113002
11. Kuhn S, Hakanson U, Rogobete L, Sandoghdar V (2006) Enhancement of single-molecule fluorescence using a gold nanoparticle as an optical nanoantenna. Phys Rev Lett 97(1):017402
12. Aslan K et al (2005) Metal-enhanced fluorescence: an emerging tool in biotechnology. Curr Opin Biotechnol 16(1):55–62
13. D'Agostino S et al (2009) Enhanced fluorescence by metal nanospheres on metal substrates. Opt Lett 34(15):2381–2383
14. Dragan AI et al (2010) Metal-enhanced picogreen fluorescence: application for double-stranded DNA quantification. Anal Biochem 396(1):8–12
15. Mackowski S et al (2008) Metal-enhanced fluorescence of chlorophylls in single light-harvesting complexes. Nano Lett 8(2):558–564
16. Matveeva EG et al (2007) Metal particle-enhanced fluorescent immunoassays on metal mirrors. Anal Biochem 363(2):239–245
17. Pribik R et al (2009) Metal-enhanced fluorescence (MEF): physical characterization of silver-island films and exploring sample geometries. Chem Phys Lett 478(1–3):70–74
18. Dragan AI et al (2011) Two-color, 30 second microwave-accelerated metal-enhanced fluorescence DNA assays: a new Rapid Catch and Signal (RCS) technology. J Immunol Methods 366(1–2):1–7
19. Pernice WHP (2010) Finite-difference time-domain methods and material models for the simulation of metallic and plasmonic structures. J Comput Theor Nanosci 7(1):1–14
20. Stoermer RL, Keating CD (2006) Distance-dependent emission from dye-labeled oligonucleotides on striped Au/Ag nanowires: effect of secondary structure and hybridization efficiency. J Am Chem Soc 128(40):13243–13254